

**INORGANICA CHIMICA ACTA 409: pp. 465-471. (2014)****The solvation and redox behavior of mixed ligand copper(II) complexes of acetylacetonate and aromatic diimines in ionic liquids**

Patrique Nunes,<sup>a,b</sup> Nóra Nagy,<sup>c</sup> Elisabete C.B.A. Alegria,<sup>a,d</sup> Armando J.L. Pombeiro,<sup>a</sup> Isabel Correia<sup>a,\*</sup>

<sup>a</sup> Centro de Química Estrutural, Instituto Superior Técnico, Av. Rovisco Pais 1, 1049-001 Lisbon, Portugal. Fax: +351 2 1846445; Tel: +351 2 18419268, Email:

[icorreia@ist.utl.pt](mailto:icorreia@ist.utl.pt)

<sup>b</sup> UCQR, Instituto Superior Técnico, Polo de Loures, Campus Tecnológico e Nuclear, Estrada Nacional 10, Km 139,7 - 2695-066 Bobadela LRS - Portugal

<sup>c</sup> Institute of Structural Chemistry, Chemical Research Center, Hungarian Academy of Sciences, Pusztaszeri út 59-67, H-1025 Budapest, Hungary

<sup>d</sup> Departamento de Engenharia Química, ISEL, R. Conselheiro Emídio Navarro, 1950-062 Lisbon, Portugal

**Abstract**

The behavior of two cationic copper complexes of acetylacetonate and 2,2'-bipyridine or 1,10-phenanthroline, Cu(acac)(bipy)Cl (**1**) and Cu(acac)(phen)Cl (**2**), in organic solvents and ionic liquids, was studied by spectroscopic and electrochemical techniques. Both complexes showed solvatochromism in ionic liquids although no correlation with solvent parameters could be obtained. By EPR spectroscopy rhombic spectra with well-resolved superhyperfine structure were obtained in most ionic liquids. The spin Hamiltonian parameters suggest a square planar geometry with coordination of the ionic liquid anion. The redox properties of the complexes were investigated by cyclic voltammetry at a Pt electrode (d = 1 mm) in bmimBF<sub>4</sub> and bmimNTf<sub>2</sub> ionic liquids and showed that complexes **1** and **2** can be

electrochemically reduced in these ionic media. The results show that both copper(II) complexes are reduced at more negative potentials when cyclic voltammeteries are conducted in ionic liquids instead of organic solvents, thus being more difficult to reduce in these ionic solvents. This is in agreement with the EPR characterization, which shows lower  $A_z$  and higher  $g_z$  values for the complexes dissolved in ionic liquids, than in organic solvents, due to higher electron density at the Copper center. The anion basicity order obtained by EPR is  $\text{NTf}_2^-$ ,  $\text{N}(\text{CN})_2^-$ ,  $\text{MeSO}_4^-$  and  $\text{Me}_2\text{PO}_4^-$ , which agrees with previous determinations.

*Keywords:* cationic copper complexes, ionic liquids, EPR, cyclic voltammetry.

## Introduction

Room temperature ionic liquids are considered alternative substitutes to volatile organic solvents due to having properties like very low vapor pressure, high thermal stability, broad liquid range, and high solvation power for a broad range of organic compounds and catalysts, which include Lewis acids.<sup>1</sup> In catalysis the coordination ability of the ionic liquid is an essential property since in many catalytic reactions the transition metal complex needs to coordinate the substrate for the reaction to occur. It has been shown that this is mainly related to the ionic liquid anion.<sup>2, 3</sup> Many techniques have been used to study the coordination ability of the ionic liquid anion, the simplest one being the measurement of the Vis spectra of solvatochromic dyes. Particularly, the following transition metal complexes have been used as solvatochromic probes:  $[\text{Fe}(\text{phen})_2(\text{CN})_2]\text{ClO}_4$ ,<sup>4</sup>  $[\text{Cu}(\text{acac})(\text{tmen})][\text{B}(\text{Ph})_4]$ ,<sup>2, 3</sup>  $[\text{Ni}(\text{acac})(\text{tmen})][\text{B}(\text{Ph})_4]$ <sup>5</sup> and  $[\text{Mn}(\text{NTf}_2)_2]$ <sup>6</sup> phen = 1,10-phenanthroline, acac =

acetylacetonate, tmen = N,N,N',N'-tetramethylethylenediamine, B(Ph)<sub>4</sub> = tetraphenylborate<sup>7</sup>.

For [Cu(acac)(tmen)][B(Ph)<sub>4</sub>] the visible electronic absorption bands can be correlated with solvent donor numbers.<sup>8</sup> A shift in the lowest energy band (in the Vis range) is observed and is a result of the d-orbital splitting of copper(II) when the complex becomes penta- or hexa-coordinated. In ionic liquids the shift was independent of the nature of the cation and was only dependent on the IL anion.<sup>3</sup> A basicity order was obtained for the studied IL anions: PF<sub>6</sub><sup>-</sup> < NTf<sub>2</sub><sup>-</sup> < OTf<sup>-</sup>.

Our group reported on the structural characterization of VO(acac)<sub>2</sub> in imidazolium ionic liquids, and showed that the vanadium complex is solvatochromic in the selected ionic liquids and behaves as in organic solvents, evidencing coordination of the ionic liquid anion in the solvents with higher coordinating ability.<sup>9</sup> The Lewis basicity order obtained in this study was: PF<sub>6</sub><sup>-</sup> < NTf<sub>2</sub><sup>-</sup> < OTf<sup>-</sup> ≈ MeCO<sub>2</sub><sup>-</sup> < MeSO<sub>4</sub><sup>-</sup> < BF<sub>4</sub><sup>-</sup> ≈ N(CN)<sub>2</sub><sup>-</sup> < Me<sub>2</sub>PO<sub>4</sub><sup>-</sup>, similar to the one obtained by Wassercheidt *et al.*<sup>2</sup>

In this paper we take our studies further and investigate the effect of the solvent on the Visible and EPR parameters of mixed cationic complexes containing acetylacetonate and aromatic diimines.

Several X-ray structures have been published for cationic mixed ligand copper(II) complexes of the type Cu(acac)(NN)X, in which NN is 1,10-phenanthroline (phen) or 2,2'-bipyridine (or a derivative) and X is an anion.<sup>10-15</sup> The X-ray structures of two complexes containing acac and phen (or 2,9-dimethyl-1,10-phenanthroline) and NO<sub>3</sub><sup>-</sup> as counterion, show that in both complexes the copper atom has an approximate square pyramidal coordination geometry.<sup>12</sup> Another phen complex, in which the counterion is ClO<sub>4</sub><sup>-</sup>, shows the same geometry, also with the anion

occupying the axial position.<sup>13</sup> A structure containing water in the axial position and  $\text{NO}_3^-$  as counterion was found for  $[\text{Cu}(\text{acac})(\text{bipy})(\text{H}_2\text{O})]\text{NO}_3$ , while for the analogous 1,10-phenanthroline complex the  $\text{Br}^-$  occupied the axial position, instead of the water molecule.<sup>14</sup> Complexes containing the bulky  $\text{BPh}_4^-$  show coordination of solvent molecules in the apical position.<sup>15</sup>

These type of complexes, generally known as CASIOPEINAS<sup>®</sup>, have been widely studied due to their potentially useful pharmacological properties, such as cytotoxic and antineoplastic.<sup>16, 17</sup> However, their characterization in solution is still underdeveloped. Moreover, ionic liquids are being considered as alternative pharmaceutical solvents for poorly water-soluble model drugs<sup>18</sup> and also as Active Pharmaceutical Ingredients.<sup>18, 19</sup> Therefore, the structural characterization of the selected copper complexes in ionic liquids is an issue of utmost importance.

It is well known that the chemical bonding in a compound is influenced by the solvent. Electron paramagnetic resonance (EPR) is a valuable spectroscopic tool for the determination of the coordination environment in paramagnetic metal complexes. Copper(II), having one unpaired electron in a  $d^9$  electronic configuration and a nuclear spin of  $3/2$  is a suitable metal ion to be studied by this technique. Also, the copper(II) unpaired electron occupies an orbital which points directly to the equatorial ligands, therefore, often interaction of the electron with the nuclear spin of donor atoms such as  $^{14}\text{N}$  is observed, providing a way to determine the ligand environment around the Cu(II) metal center in solution.

In this report we present the structural characterization of  $\text{Cu}(\text{acac})(\text{bipy})\text{Cl}$  and  $\text{Cu}(\text{acac})(\text{phen})\text{Cl}$  [bipy = 2,2'-bipyridine and phen = 1,10-phenanthroline] by Vis and EPR spectroscopies, in organic solvents and ionic liquids. Well-resolved EPR

spectra for the copper complexes were obtained in most solvents. Their redox behavior in selected organic solvents and ionic liquids is also evaluated.

## **Results and discussion**

*Characterization of the ionic liquids* – The components of the ionic liquids chosen for this study are depicted in Scheme 1. Syntheses of the ionic liquids were performed under anaerobic conditions using standard Schlenk techniques. The preparations and spectral data of the ionic liquids have been described elsewhere<sup>20</sup>. The procedure used in its preparation and purification (washing with water, addition of charcoal, and filtration through alumina) afforded colorless liquids, suitable for spectroscopic studies. The analytic characterization showed the absence of impurities, such as residual chloride, which might change considerably their solvation properties. Before using the ILs were dried for at least 48h under vacuum at 50°C. The water content of the dried ionic liquids was measured by Karl Fischer coulometer analysis. For the hydrophobic ILs (p.e. bmimBF<sub>4</sub>) the values did not exceed 350 ppm but for the most hygroscopic they are ca. 1500 ppm, which in terms of water concentration corresponds to 0.08M.

### *Scheme 1*

*Characterization of the copper(II) complexes* – The copper(II) complexes (see Scheme 1) were prepared by mixing the ligands and CuCl<sub>2</sub> in alcohols. The structural characterization by elemental analysis and FTIR (data included in the experimental section) confirmed its formulation.

Both complexes were also characterized by electronic absorption spectroscopy with its spectra being measured in a wide range of organic solvents, which are included in

the SI. Overall, the complexes show two or three bands in the Vis region (in some cases they are overlapped). Being a  $3d^9$  metal center, copper(II) is usually subject to Jan-Teller distortion. In square planar or octahedral complexes the unpaired electron occupies the  $d_{x^2-y^2}$  orbital, which has its lobes pointing directly to the equatorial ligands, along the x and y axis of the molecule. The correlation of the low energy absorption maximum with the Kamlet Taft (KT) solvent parameters in organic solvents, showed that although in most cases the fitting parameters were not satisfactory, there were clear correlations with  $\alpha$ , the hydrogen bond acidity (see SI1).

In ionic liquids it was not possible to obtain any correlation with the KT solvent parameters, which seems to indicate that the solvation process depends on several parameters, but since the number of solvents is limited, it is not possible to obtain any correlation with more than one parameter. **Figure 1** shows the Vis electronic spectra obtained for Cu(acac)(bipy)Cl dissolved in selected ionic liquids. Both complexes are soluble in most ILs and the most solvathochromic complex is the bipy derivative, complex **1**, which presents a variation of ca. 170 nm in the position of the absorption maximum for the lower energy band. **Table 1** resumes the collected data, which is also included in graphical form in the supplemental information.

*Figure 1*

*Table 1*

*EPR in organic solvents* – The EPR spectra of Cu(acac)(bipy)Cl in organic solvents were measured both at room temperature and 77K. The EPR spectra of Cu(acac)(phen)Cl were measured only at 77K. All spectra were simulated with a computed program developed by Rockenbauer and Koretz.<sup>21</sup> At room temperature

the spectra measured for complex Cu(acac)(bipy)Cl present the expected four-lines splitting and the line widths vary with  $m_l$ , with the high field line being narrower and more intense than the lower field lines. Table 2 presents the spin Hamiltonian parameters obtained by simulation.

The anisotropic spectra measured at liquid nitrogen temperature (77K) are much more resolved and informative. The unpaired electron of the copper center occupies an orbital that points directly to the equatorial ligands and consequently there may be interaction of the electron with the nuclear spin of the  $^{14}\text{N}$  donor atoms. This is commonly known as superhyperfine (shf) coupling interaction. So, when a nitrogen atom is coordinated to Cu(II) an additional splitting of the hyperfine lines may be observed. Each hyperfine signal can be further split into  $2n+1$  signals ( $l$  is the nuclear magnetic moment and  $n$  is the number of the corresponding nuclei), each separated by a superhyperfine constant. Thus, one  $^{14}\text{N}$  donor will give rise to a 1:1:1 triplet, and two  $^{14}\text{N}$  donors to a 1:2:3:2:1 quintet. When present, the shf structure is usually visible in the  $xy$  component as the  $z$  component is usually undetected due to line broadening. However, for the studied complexes, in some cases the shf coupling was observed in both components: *p.e.* the spectrum of Cu(acac)(bipy)Cl in ethanol (see SI, Figure SI5) or in bbimNTf<sub>2</sub>.

Most spectra were simulated considering rhombic symmetry for the  $g$  and  $A$  tensors; and when shf structure was present, rhombic shf tensors were also used for the two nitrogen atoms. When the spectra presented the parallel copper shf well resolved it was also possible to determine the nitrogen shf coupling in the  $z$  direction. The spectra were simulated with Gaussian line shape (in most cases) and the line width

described as dependent, *i.e* the line width changes with the orientation (parallel or antiparallel direction) and with the magnetic quantum number.

The spectra measured at 77K in CH<sub>3</sub>CN, H<sub>2</sub>O and DMSO are not resolved, and only a singlet is observed, due to strong magnetic interactions between the copper centers in these solvents. In EtOH the spectrum shows very good resolution and shf coupling is observed also in the parallel region. The simulation of the spectra retrieved the spin-Hamiltonian parameters included in Table 2. These are roughly in agreement with previously published values for similar complexes.<sup>10, 13</sup> In DMF complex **1** shows two species. We were able to simulate both of them, however its assignment is not straightforward. The one with the higher  $A_z$  probably correspond to a solvolysis species, since DMF has high coordination ability.

*EPR in ionic liquids* – The X-band EPR spectra of both complexes dissolved in a series of ionic liquids containing mostly imidazolium cations, and anions with different coordinating abilities, were measured at 77K. Figures 2 and 3 depict the spectra measured for both complexes and the spin-Hamiltonian parameters are included in Table 2. The EPR spectra seem axial however the symmetry of the complexes is lower and simulation of the spectra with rhombic parameters yielded better fittings in most cases. The spectra show well-resolved hyperfine and superhyperfine structure in the parallel (in some ILs) and perpendicular regions: in the parallel region three of four hyperfine bands are well resolved while the fourth one is overlapped by  $g_z$  features. Most spectra show similar features (except in bmimOAc) and, particularly the spectra measured in ILs containing the NTf<sub>2</sub> anion show high-resolution superhyperfine structure in the perpendicular region. However,



in these ILs (and **1** in bmimPF<sub>6</sub> and **2** in bmimBF<sub>4</sub>) an extra resonance appears at  $g \approx 1.8$ , which is, most likely, due to the presence of dimeric species. However, although spectra were also measured at  $g \approx 4$  (~1500G, forbidden transition) to detect transitions due to  $\Delta M_S = \pm 2$  (magnetic dipolar coupling between copper centers), no signals were detected.

#### *Figures 2 and 3*

In figure 4 we present the experimental and simulated spectra of complex **1** in bmimN(CN)<sub>2</sub>, which evidences the quality of the fitting and the shf resolution. The shf structure was simulated considering coupling with two <sup>14</sup>N nuclei. Overall, the nitrogen coupling shows one big and two small values, with the biggest one pointing towards the copper ion. This implies that since the complexes have two non-equivalent neighboring nitrogen donors, one of them has a large coupling in the x-axis and the other one in the y-axis. As an example, complex **1** in bmpyNTf<sub>2</sub> shows SHF coupling constants of N<sub>1</sub>:  $a_x = 5.64$  G,  $a_y = 15.19$  G and  $a_z = 5.57$  G and of N<sub>2</sub>:  $a_x = 15.19$  G,  $a_y = 6.71$  G and  $a_z = 0.01$  G. very The shf parameters for all complexes, which present SHF resolution, are quite similar.

#### *Figure 4*

Overall, for both complexes the  $A_z$  coupling constant is lower in the ionic liquids than in the organic solvents. With the  $g_z$  value the opposite is observed. Upon solvent coordination the copper-donor atom bond increases, lowering the delocalization of the electron density, and increasing the density at the copper atom. This is usually reflected in the spin Hamiltonian parameters, particularly in a decrease in  $A_z$  and an increase in  $g_z$ . Therefore we can conclude that overall the ionic liquids show higher coordinating power than the selected organic solvents.

Figure 5 shows the correlation between  $g_z$  and  $A_z$  for both complexes. Except for complex **1** in bmimOAc and complex **2** in bmimBF<sub>4</sub> a good correlation was obtained, which shows the usual trend: an increase in  $g_z$  is accompanied by a decrease in  $A_z$ . Solvents in the low right end of the graph show higher basicity, and solvents in the high left end show lower basicity. Regardless of the cation (bbim, bmim or bmpy), the NTf<sub>2</sub> anion shows the lower basicity, followed by N(CN)<sub>2</sub>, MeSO<sub>4</sub> and Me<sub>2</sub>PO<sub>4</sub>. For bmimBF<sub>4</sub> no straightforward conclusion can be taken since BF<sub>4</sub><sup>-</sup> is an anion, which theoretically has high coordination power, but due to its high water affinity, usually falls out of the correlations. The problem with bmimOAc is that more than one species is observed in the EPR spectra, since this anion has the possibility to form polymeric species with copper ions.

For all the ionic liquids in which the EPR spectra of complex **2** were measured, the hyperfine coupling constant  $A_z$  is considerably lower than for complex **1** (see Table 2). Phenanthroline and bipyridine have similar electron-donor properties (see below) but phenanthroline is a more rigid ligand than bipy. Therefore, the coordination to Cu might be less efficient in phen, due to steric constraints, increasing the Cu-donor atom bonds, and decreasing the coupling constant  $A_z$ .

### *Figure 5*

#### *Redox behavior of the complexes*

The study of the redox behavior of the complexes started with the measurement of cyclic voltammograms of pure bmimBF<sub>4</sub> and bmimNTf<sub>2</sub> at a platinum disc working electrode ( $d = 1$  mm), at room temperature. A broad reduction wave was observed at ca. 1.9 V vs. FcH/FcH<sup>+</sup>, probably due to the reduction of the bmim<sup>+</sup> cation to carbene that could be followed by dealkylation and dimerization reactions.<sup>22</sup> Upon scan

reversal, following the cathodic process, a new oxidation wave is observed at  $E_p = 0.5$  V vs. FcH/FcH<sup>+</sup>, corresponding to the oxidation of a species formed at the cathodic process. This shows that bmimBF<sub>4</sub> (and bmimNTf<sub>2</sub>) is electrochemically stable in the potential range of our study, in accordance with previous observations.<sup>23-25</sup>

The Cu(II) complexes show one first irreversible reduction process (wave I<sup>red</sup>) at potential values  $^I E_p^{\text{red}} = -0.86$  and  $-0.87$  V vs. FcH/FcH<sup>+</sup> for **1** and **2**, respectively, in bmimNTf<sub>2</sub>, and at potentials of  $^I E_p^{\text{red}} = -0.85$  and  $-0.82$  V vs. FcH/FcH<sup>+</sup> for **1** and **2**, respectively, in bmimBF<sub>4</sub>. This is followed, at a lower potential, by a second irreversible wave (wave II<sup>red</sup>) at  $^{II} E_p^{\text{red}} = -1.20$  and  $-1.18$  V vs. FcH/FcH<sup>+</sup> for **1** and **2**, respectively, in bmimNTf<sub>2</sub>, and at  $^{II} E_p^{\text{red}} = -1.23$  and  $-1.21$  V vs. FcH/FcH<sup>+</sup> for **1** and **2**, respectively, in bmimBF<sub>4</sub> (Figures 6 and 7, for complex **1** in bmimNTf<sub>2</sub> and bmimBF<sub>4</sub>, respectively). Moreover, a third reduction process is observed at ca.  $-1.6$  V, possibly due to reduction of a new species, which could also result from reaction with IL. For both complexes, **1** and **2**, the two cathodic processes (I<sup>red</sup> and II<sup>red</sup>) are believed to correspond to the Cu<sup>II</sup> → Cu<sup>I</sup> and Cu<sup>I</sup> → Cu<sup>0</sup> reduction steps.<sup>7, 26-30</sup>

#### *Figures 6 and 7*

Complexes **1** and **2** exhibit one irreversible oxidation wave (wave I<sup>ox</sup>), which is attributed to the chloride counter-ion, its potential value being in the range observed for the same process in bmimPF<sub>6</sub>.<sup>31</sup> Upon scan reversal, following the cathodic processes (I<sup>red</sup> and II<sup>red</sup>), two new oxidation waves appear (II<sup>ox</sup> and III<sup>ox</sup>, Figures 6 and 7, for complex **1**), conceivably due to the oxidation of new species formed at those cathodic processes.

The similarity of the first reduction potential values observed for **1** and **2** is indicative of a similar electron-donor character of the 2,2'-bipyridine and 1,10-phenanthroline ligands. In fact, in accordance with the values<sup>32-34</sup> of the electrochemical Lever  $E_L$  parameter (the stronger that character, the lower  $E_L$ ) for these ligands, both exhibit an  $E_L$  value of 0.26 V vs. NHE. Moreover, the considerable lower  $E_L$  parameter of acac ( $E_L = -0.08$  V)<sup>32-34</sup>, is indicative of a much stronger electron-donor ability of acac in comparison with the bipy and phen ligands.

Solutions containing different concentrations of **1** in bmimBF<sub>4</sub> were studied by CV, showing a linear dependence of  $i_p$  with the concentration (See SI, Figure SI7). For low concentrations (ca. 1 mM) no significant waves were observed for **1** and **2**. The influence of different scan rates ( $v$ ) on the cyclic voltammograms was studied and showed that the dependence of the current intensity of the cathodic peaks of **I**<sup>red</sup> and **II**<sup>red</sup> are linear in the studied scan rate range 20-1000 mVs<sup>-1</sup> (Figure 8). The resulting voltammograms show that the anodic waves **I**<sup>ox</sup> and **II**<sup>ox</sup> are related to **I**<sup>red</sup> and **II**<sup>red</sup> and hence attributed to the oxidation of reduced specie formed in those cathodic processes.

### Figure 8

For comparative purposes the redox properties of both Cu(II) complexes were also investigated by cyclic voltammetry in 0.2 M [<sup>n</sup>Bu<sub>4</sub>N][BF<sub>4</sub>]/(CH<sub>2</sub>Cl<sub>2</sub> or NCMe) solutions, at 25°C, and the measured redox potentials (in V vs. FcH/FcH<sup>+</sup>) are given in Table 3. Complexes **1** and **2** show one first irreversible reduction process (wave **I**<sup>red</sup>, SI, Figure SI9 for **1** and **2**, in NCMe) at potentials values  $^1E_p^{red} = -0.60$  and  $-0.57$  V vs. FcH/FcH<sup>+</sup> for **1** and **2**, in CH<sub>2</sub>Cl<sub>2</sub> (and at potentials values  $^1E_p^{red} = -0.78$  and  $-0.55$  V vs. FcH/FcH<sup>+</sup> for **1** and **2**, in NCMe), followed, at a lower potential, by a second

single-electron irreversible wave (wave  $\text{II}^{\text{red}}$ , SI, Figure SI9 for **1** and **2**, in NCMe) at  $^{\text{II}}E_{\text{p}}^{\text{red}} = -1.02$  and  $-0.93\text{V}$  vs. FcH/FcH<sup>+</sup> in CH<sub>2</sub>Cl<sub>2</sub> (and at  $^{\text{II}}E_{\text{p}}^{\text{red}} = -1.09$  and  $-0.86$  V vs. FcH/FcH<sup>+</sup> in NCMe).

The exhaustive controlled-potential electrolysis to measure the number of electrons involved in each redox process was not possible to do due to the fast passivation of the cathode, probably owing to the formation of an insoluble Cu<sup>0</sup> compound at the electrode surface (see Figure SI9a in SI, for complex **1**).

Complexes **1** and **2** also exhibit one irreversible oxidation wave ( $\text{I}^{\text{ox}}$ ) attributed to the chloride counter-ion oxidation. This fact is supported by the independently measured value ( $E_{\text{p}}^{\text{ox}} = 0.64$  V vs. FcH/FcH<sup>+</sup>, in NCMe) of the irreversible oxidation wave of benzyltriethylammonium chloride under the same experimental conditions, and confirmed by the increase of the current intensity of the wave  $\text{I}^{\text{ox}}$  upon addition of this chloride salt to a solution of complex **1** and **2**, in NCMe. Upon scan reversal, following the cathodic processes ( $\text{I}^{\text{red}}$  and  $\text{II}^{\text{red}}$ ), two new oxidation waves appear ( $\text{II}^{\text{ox}}$  and  $\text{III}^{\text{ox}}$ , Figures SI9a for complex **1**), conceivably due to the oxidation of new species formed at those cathodic processes.

As can be observed in this study, both copper(II) complexes, **1** and **2**, are reduced at more negative potentials when cyclic voltammeteries are conducted in ionic liquids instead of organic solvents, thus being more difficult to reduce in these ionic solvents. This fact could be related with the slower reduction kinetics<sup>26</sup> in the ionic liquids in comparison with the organic solvents, in accord, e.g. with the expected lower diffusion coefficients of the electroactive species in IL's, highly influenced by the higher viscosity and large size of constituent ions in this ionic medium.<sup>35</sup>

The peak potential difference,  $\Delta E_p$ , between e.g. the first cathodic process ( $I^{\text{red}}$ ), is slightly higher in bmimNTf<sub>2</sub> ( $\Delta E_p = 0.86$  and  $0.87$  V for **1** and **2**, respectively, Table 3) in comparison with bmimBF<sub>4</sub> ( $\Delta E_p = 0.85$  and  $0.82$  V for **1** and **2**, respectively, Table 3). However, the difference is not significant, so it is not possible, in our case, to check a possible correlation of the type reported for the ferrocenes dissolved in various ionic liquids,<sup>36, 37</sup> for which a clear linear correlation was observed between the peak potential difference  $\Delta E_p$  as a function of the molecular volume of ionic liquids anions (the potential difference increasing with the size of anions).

### Conclusions

The conducted analytical studies show that the cationic copper complexes behave in ionic liquids as in common organic solvents. The structural characterization done by spectroscopic and electrochemical techniques evidences the influence of the ionic liquid anion in the solvation of the complexes. The EPR parameters obtained in ionic liquids are of the same order as the ones measured in alcohols. Overall, the EPR characterization suggests that the ionic liquids have higher coordinating ability than the organic solvents. The following anionic basicity order was obtained: NTf<sub>2</sub><sup>-</sup>, N(CN)<sub>2</sub><sup>-</sup>, MeSO<sub>4</sub><sup>-</sup> and Me<sub>2</sub>PO<sub>4</sub><sup>-</sup>.

## Experimental

*Materials and reagents* - All chemicals used were of analytical reagent grade. 1-Methylimidazole was purchased from Acros Organics and distilled from potassium hydroxide; 1-chlorobutane was purchased from Acros Organics and distilled from phosphorus pentoxide. Lithium bis(trifluoromethylsulfonyl)imide [Li(NTf<sub>2</sub>)] and lithium trifluoromethanesulfonate [Li(OTf)] were purchased from Apollo Scientific and used as received. All syntheses and sample preparations were performed under anaerobic conditions using standard Schlenk techniques. The preparation and spectral data of the ionic liquids have been described elsewhere.

### *Synthesis of the complexes*

Cu(acac)(bipy)Cl (**1**)- The complex was prepared according to the following procedure: 103  $\mu$ L (1.0 mmol) of acetylacetone were mixed with 0.1569g (1.0 mmol) of 2,2'-bipyridine in 10 mL of ethanol. Anhydrous CuCl<sub>2</sub> (0.1360g, 1.00mmol) dissolved in 25 mL of ethanol were slowly added. The pH was set to ca. 8.5 with NaOH 1M. The reaction mixture was stirred for 30 minutes at room temperature, after which it was filtered to remove the solids. After a week of slow evaporation dark blue crystals were obtained. Yield: 58.5% (0.445 g). Anal. Calcd. For C<sub>16</sub>H<sub>18</sub>N<sub>2</sub>O<sub>2</sub>CuCl•1.2H<sub>2</sub>O: C, 50.9; H, 5.0; N, 7.4. Found: C, 50.7; H, 5.1; N, 7.8. IR (KBr disk, cm<sup>-1</sup>): 3420 [ $\nu$  (O-H)], 3043 [ $\nu$  (C-H)<sub>ar</sub>], 1581 [ $\nu$  (C=O)] for deprotonated

acetylacetonate, 1523 [ $\nu$  (C=C)], 791, wagging mode of coordinated water molecule. 449 [ $\nu$  (Cu-O)].

Cu(acac)(phen)Cl (**2**) - The complex was prepared by the procedure described above, in which bipy was replaced by 1,10-phenanthroline and instead of ethanol we used methanol. Green crystals were obtained. Yield: 68% (0.322g). Anal. Calcd. for  $C_{17}H_{15}N_2O_2CuCl \cdot 2H_2O$ : C, 48.6; H, 4.7; N, 6.7. Found: C, 48.4; H, 4.6; N, 6.9. IR (KBr disk,  $cm^{-1}$ ): 3450 [ $\nu$  (O-H)], 3044 [ $\nu$  (C-H)<sub>ar</sub>], 2988 and 2927 [ $\nu$  (C-H)<sub>alif</sub>], 1589 [ $\nu$  (C=O)], 1522 [ $\nu$  (C=C)], 455 [ $\nu$  (Cu-O)].

*Instruments* -  $^1H$  NMR spectra were recorded on a Bruker 300 or 400 MHz spectrometer. UV-vis spectra were recorded on a Perkin-Elmer UV-visible Lambda 35 spectrophotometer and the temperature was controlled with a Peltier controller from Perkin-Elmer. The EPR spectra were recorded either at 77 K (on glasses made by freezing solutions in liquid nitrogen) or at room temperature with a Bruker ESP 300E X-band spectrometer. The electrochemical experiments were performed on an EG&G PAR 273A potentiostat/galvanostat connected to a personal computer through a GPIB interface.

*Cyclic voltammetry* - All experiments were carried in glass cyclic voltammetry cell that was continuously purged with dinitrogen. Cyclic voltammograms were obtained in 0.2 M [ $n$ Bu<sub>4</sub>N][BF<sub>4</sub>]/CH<sub>2</sub>Cl<sub>2</sub> (or NCMe) solution, and in bmimNTf<sub>2</sub> or bmimBF<sub>4</sub> ionic liquids, at a platinum disc working electrode ( $d = 1$  mm), at room temperature. A Luggin capillary connected to a silver wire pseudo-reference electrode was used to control the working electrode potential, and a Pt wire was employed as the counter-electrode. The redox potentials of the complexes were measured by cyclic



voltammetry in the presence of ferrocene as the internal standard, and their values are quoted relative to  $[\text{Fe}(\eta^5\text{-C}_5\text{H}_5)_2]^{0/+}$  ( $\text{FcH}/\text{FcH}^+$ ) redox couple (values are given in Table 3).

**Acknowledgments** – The authors would like to thank Fundação para a Ciência e Tecnologia for funding: program CIÊNCIA 2007 and projects PTDC/QUI-QUI/098516/2008, PTDC/QUI-QUI/102150/2008 and Pest-OE/QUI/UI0100/2011.

### Figure Captions

Figure 1 – Electronic absorption spectra in the Vis region for  $\text{Cu}(\text{acac})(\text{bipy})\text{Cl}$  in selected ionic liquids. Complex concentration ca. 3mM, path length 1 cm. The spectrum in  $\text{bmimMeSO}_4$  was measured at 50°C due to the higher melting point of this IL.

Figure 2 – X-band EPR spectra measured at 77K for complex **1**,  $\text{Cu}(\text{acac})(\text{bipy})\text{Cl}$ , in selected ionic liquids.

Figure 3 – X-band EPR spectra measured at 77K for complex **2**,  $\text{Cu}(\text{acac})(\text{phen})\text{Cl}$ , in selected ionic liquids.

Figure 4 – Experimental and simulated EPR spectra of complex **1**,  $\text{Cu}(\text{acac})(\text{bipy})\text{Cl}$ , in  $\text{bmimN}(\text{CN})_2$ .

Figure 5 – Correlation between the spin Hamiltonian parameters  $A_z$  and  $g_z$  for both complexes. 1)  $\text{bmimNTf}_2$ , 2)  $\text{bmimPF}_6$ , 3)  $\text{bbimNTf}_2$ , 4)  $\text{bmpyNTf}_2$ , 5)  $\text{bmimN}(\text{CN})_2$ , 6)  $\text{bmimMeSO}_4$ , 7)  $\text{bmimBF}_4$ , 8)  $\text{bmimMe}_2\text{PO}_4$  and 9)  $\text{bmimOAc}$ .

Figure 6 - Cyclic voltammogram of complex **1**, at a Pt electrode, initiated by the cathodic sweep, in  $\text{bmimNTf}_2$  ( $\nu = 200 \text{ mVs}^{-1}$ ).  $[\text{Complex } \mathbf{1}] = 5.1 \text{ mM}$ .

Figure 7 - Cyclic voltammogram of complex **1**, at a Pt electrode, initiated by the cathodic sweep, in  $\text{bmimBF}_4$  ( $\nu = 200 \text{ mVs}^{-1}$ ).  $[\text{Complex } \mathbf{1}] = 50 \text{ mM}$ .

Figure 8 - Linear correlation between the reduction peak current of  $I^{\text{red}}$  vs. the square root of the scan rates for the CVs presented in Figure S18.

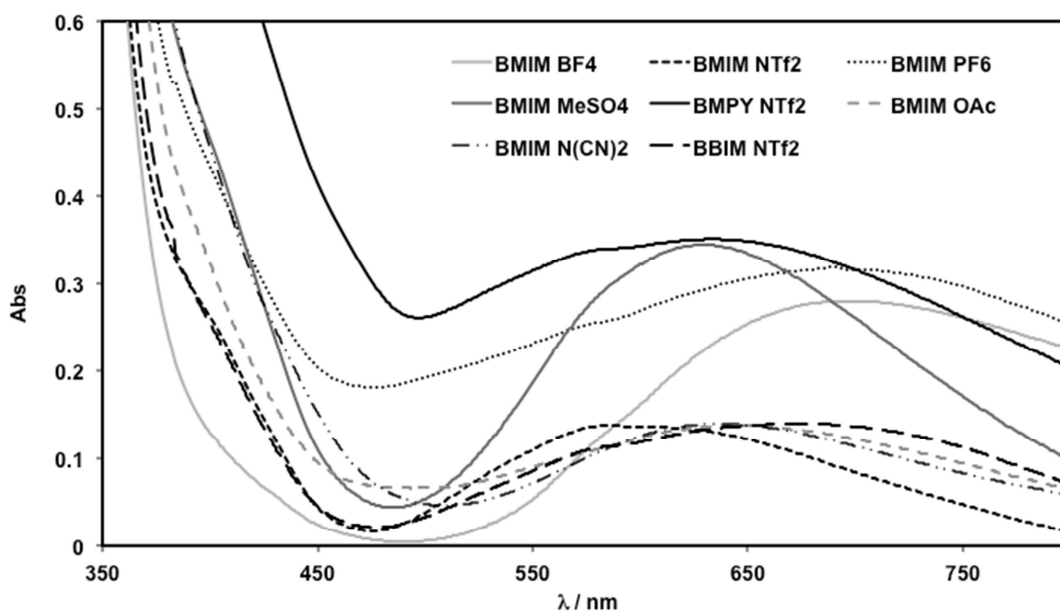


Figure 1 – Electronic absorption spectra in the Vis region for Cu(acac)(bipy)Cl in selected ionic liquids. Complex concentration ca. 3mM, path length 1 cm. The spectrum in bmimMeSO<sub>4</sub> was measured at 50°C due to the higher melting point of this IL.

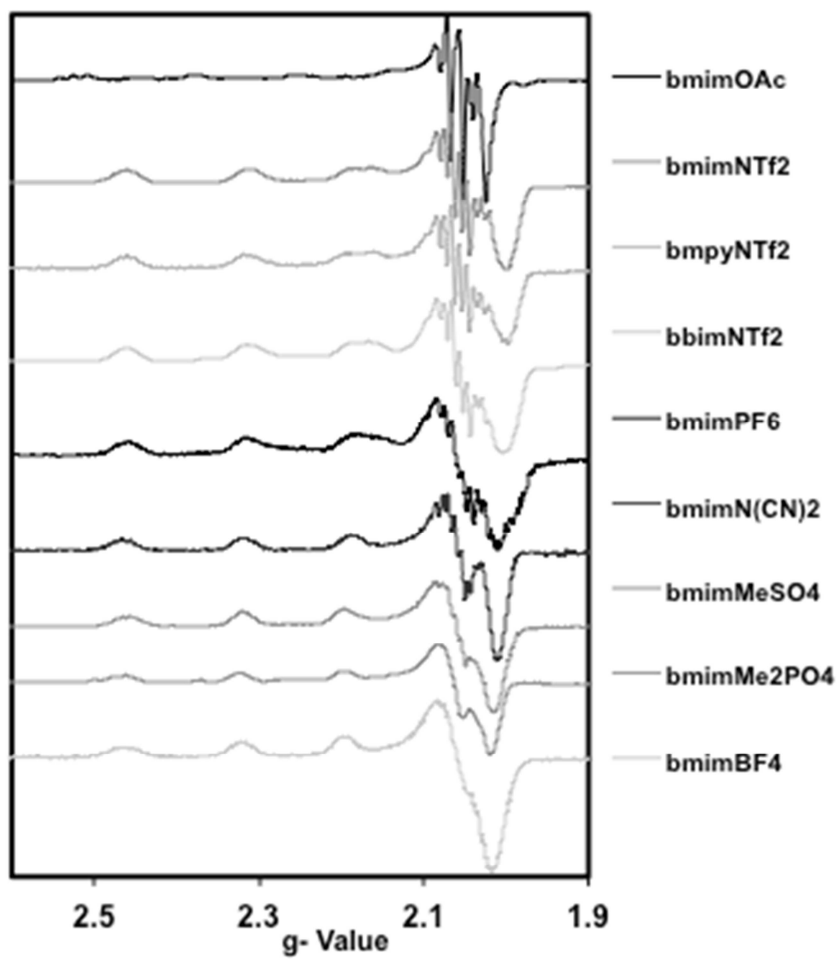


Figure 2 – X-band EPR spectra measured at 77K for complex 1, Cu(acac)(bipy)Cl, in selected ionic liquids.

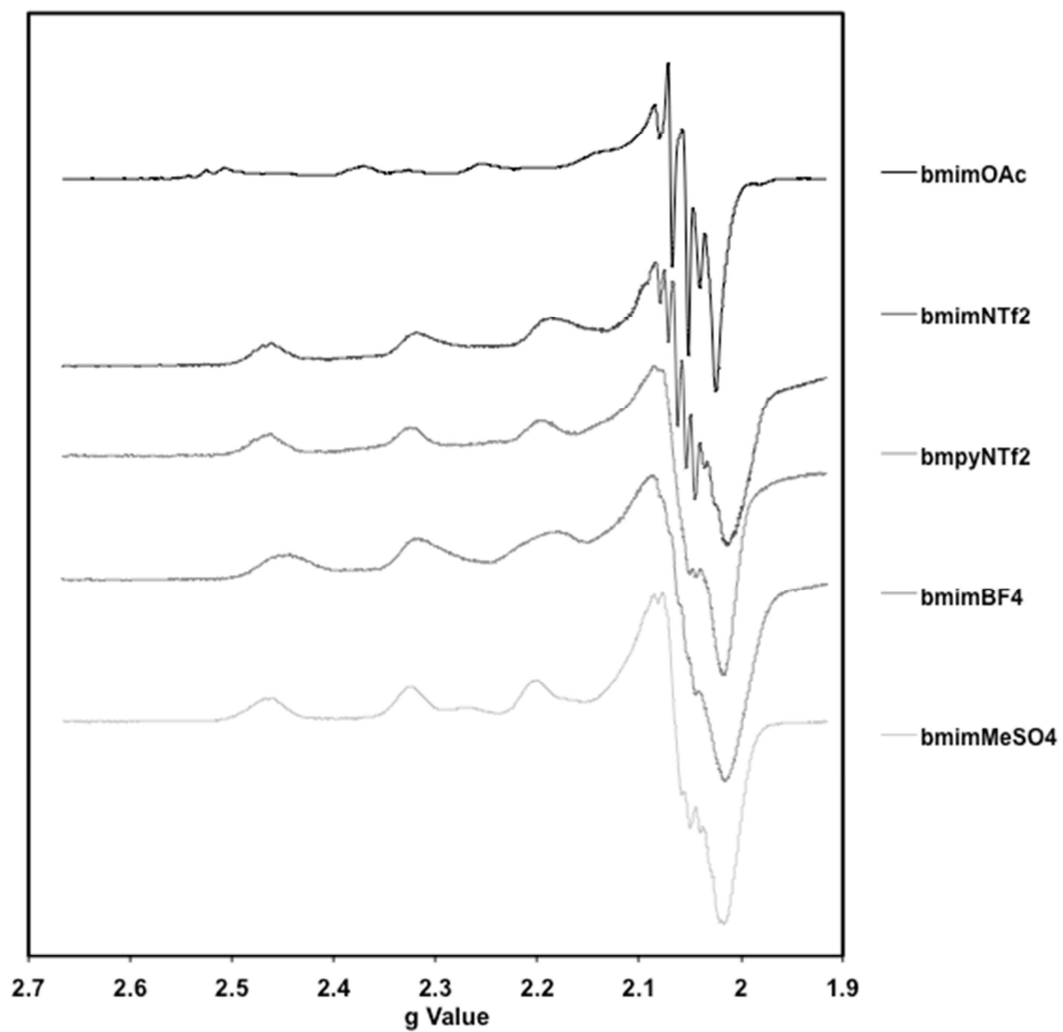


Figure 3 – X-band EPR spectra measured at 77K for complex **2**, Cu(acac)(phen)Cl, in selected ionic liquids.

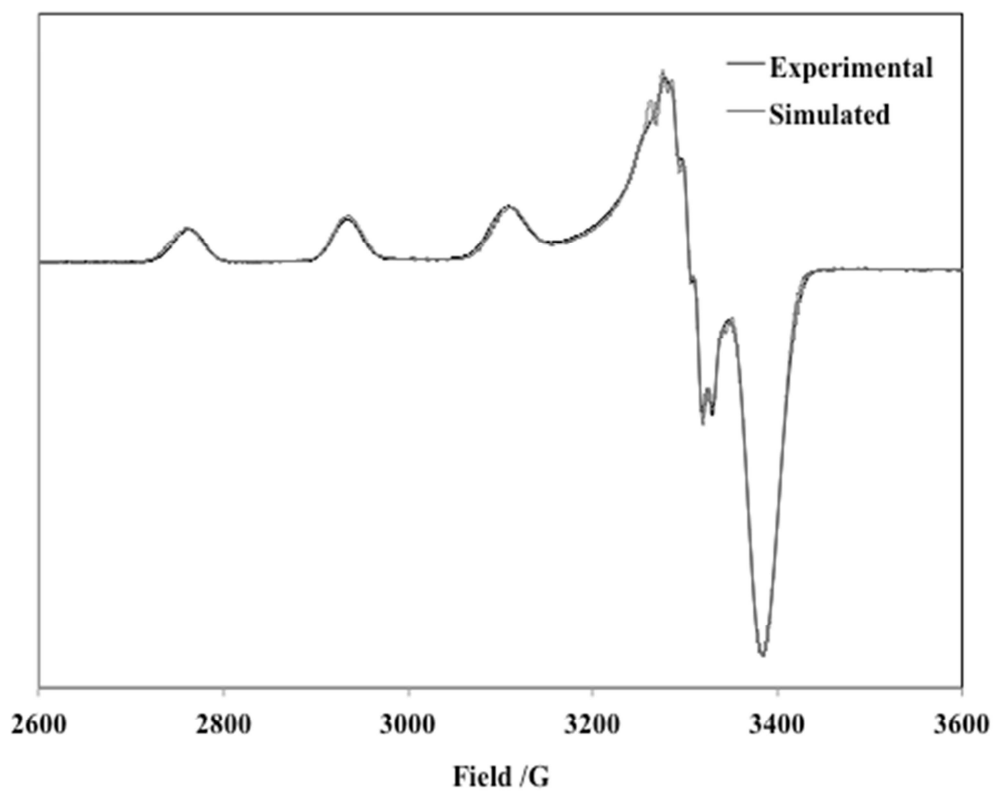


Figure 4 – Experimental and simulated EPR spectra of complex **1**, Cu(acac)(bipy)Cl, in bmimN(CN)<sub>2</sub>.

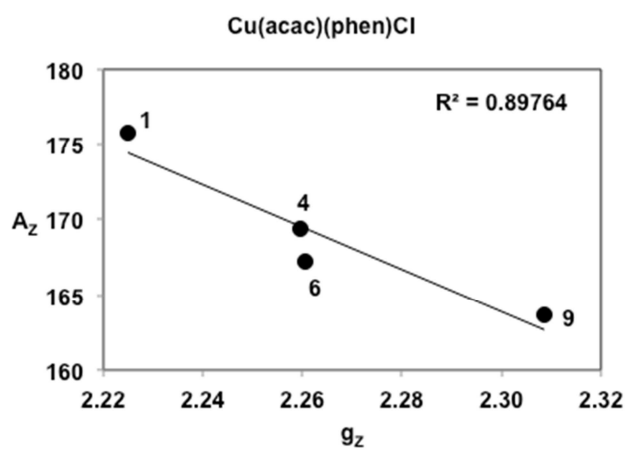
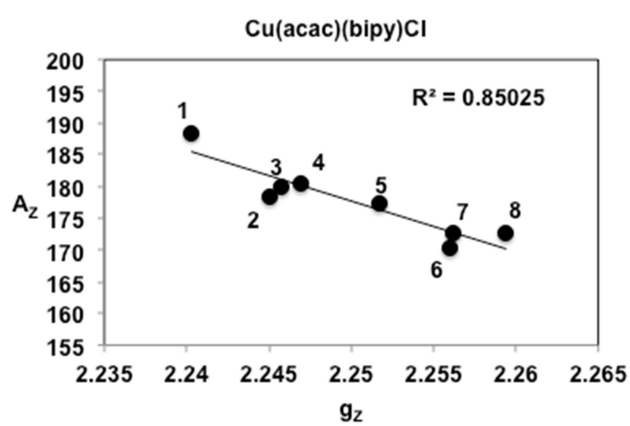


Figure 5 – Correlation between the spin Hamiltonian parameters  $A_z$  and  $g_z$  for both complexes. 1) bmimNTf<sub>2</sub>, 2) bmimPF<sub>6</sub>, 3) bbimNTf<sub>2</sub>, 4) bmpyNTf<sub>2</sub>, 5) bmimN(CN)<sub>2</sub>, 6) bmimMeSO<sub>4</sub>, 7) bmimBF<sub>4</sub>, 8) bmimMe<sub>2</sub>PO<sub>4</sub> and 9) bmimOAc.

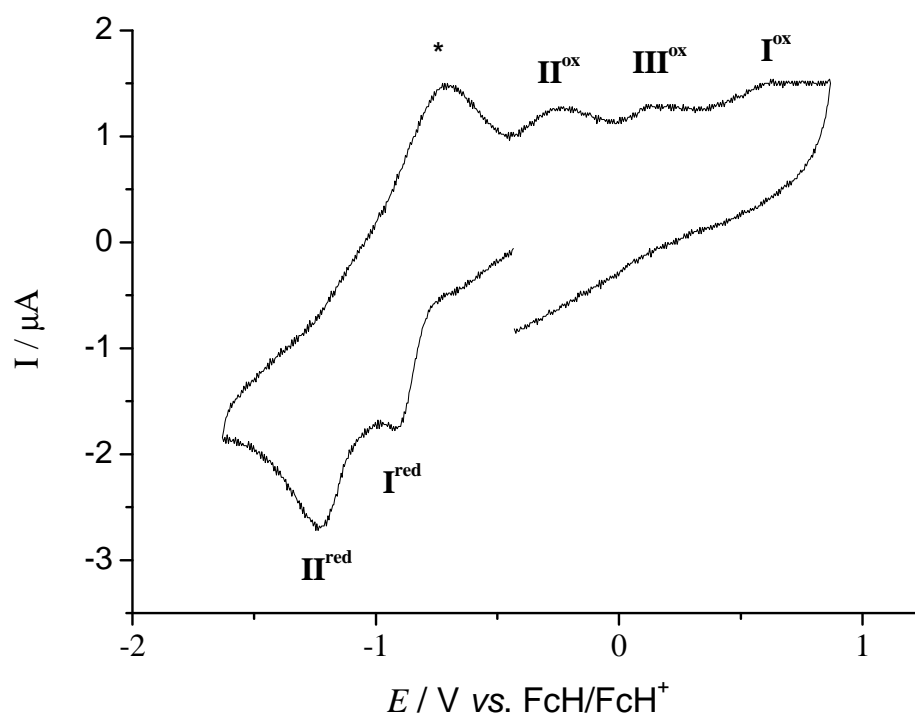


Figure 6 - Cyclic voltammogram of complex 1, at a Pt electrode, initiated by the cathodic sweep, in  $\text{bmimNTf}_2$  ( $\nu = 200 \text{ mVs}^{-1}$ ).  $[\text{Complex 1}] = 5.1 \text{ mM}$ .



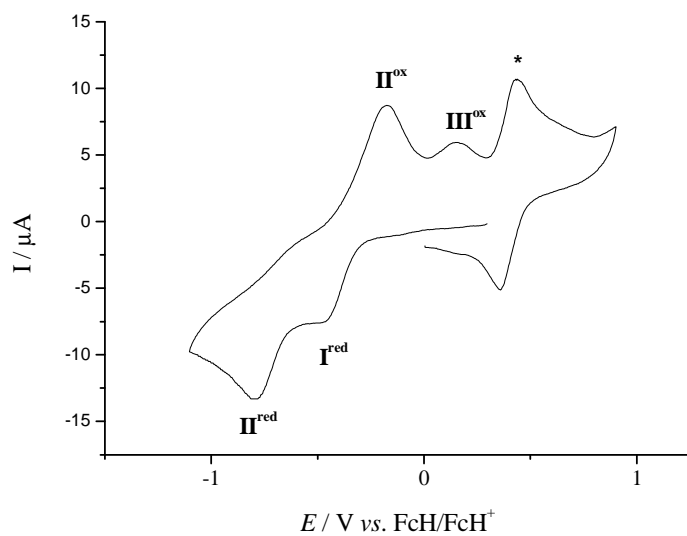


Figure 7 - Cyclic voltammogram of complex **1**, at a Pt electrode, initiated by the cathodic sweep, in bmimBF<sub>4</sub> ( $\nu = 200 \text{ mVs}^{-1}$ ). [Complex **1**] = 50 mM.

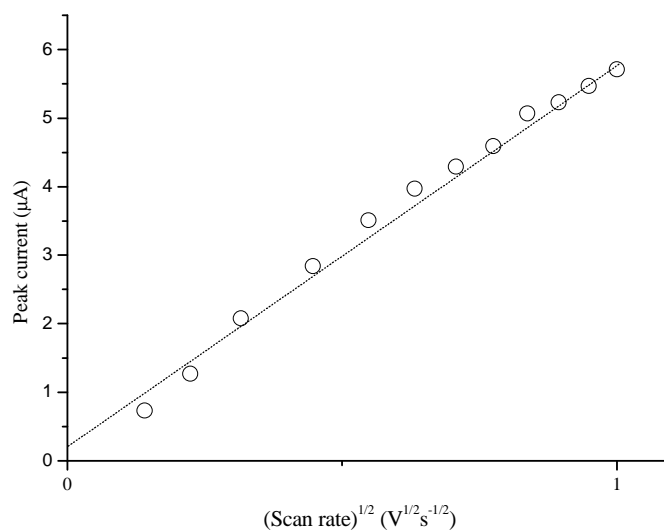


Figure 8 - Linear correlation between the reduction peak current of  $I^{\text{red}}$  vs. the square root of the scan rates for the CVs presented in Figure S18.

1. T. Welton, *Chem Rev*, 1999, **99**, 2071-2083.
2. P. Wasserscheid, C. M. Gordon, C. Hilgers, M. J. Muldoon and I. R. Dunkin, *Chem Commun*, 2001, 1700-1700.
3. M. J. Muldoon, C. M. Gordon and I. R. Dunkin, *J Chem Soc Perk T 2*, 2001, 433-435.
4. R. Lungwitz, M. Friedrich, W. Linert and S. Spange, *New J Chem*, 2008, **32**, 1493-1499.
5. J. Bartosik and A. V. Mudring, *Phys Chem Chem Phys*, 2010, **12**, 4005-4011.
6. S. Pitula and A. V. Mudring, *Phys Chem Chem Phys*, 2010, **12**, 7056-7063.
7. P. Y. Chen and I. W. Sun, *Electrochim Acta*, 1999, **45**, 441-450.
8. I. Persson, *Pure Appl Chem*, 1986, **58**, 1153-1161.

9. I. Correia, A. Mota, J. P. Hallett and M. L. Kuznetsov, *Phys Chem Chem Phys*, 2011, **13**, 15094-15102.
10. A. Tovar-Tovar, L. Ruiz-Ramirez, A. Campero, A. Romerosa, R. Moreno-Esparza and M. J. Rosales-Hoz, *J Inorg Biochem*, 2004, **98**, 1045-1053.
11. O. O. E. Onawumi, O. A. Odunola, E. Suresh and P. Paul, *Inorg Chem Commun*, 2011, **14**, 1626-1631.
12. A. Paulovicova, U. El-Ayaan and Y. Fukuda, *Inorg Chim Acta*, 2001, **321**, 56-62.
13. C. C. Su, S. P. Wu, C. Y. Wu and T. Y. Chang, *Polyhedron*, 1995, **14**, 267-275.
14. O. O. E. Onawumi, O. O. P. Faboya, O. A. Odunola, T. K. Prasad and M. V. Rajasekharan, *Polyhedron*, 2008, **27**, 113-117.
15. R. Horikoshi, Y. Funasako, T. Yajima, T. Mochida, Y. Kobayashi and H. Kageyama, *Polyhedron*, 2013, **50**, 66-74.
16. L. Becco, A. Rodriguez, M. E. Bravo, M. J. Prieto, L. Ruiz-Azuara, B. Garat, V. Moreno and D. Gambino, *J Inorg Biochem*, 2012, **109**, 49-56.
17. M. Avelar and A. Martinez, *J Mex Chem Soc*, 2012, **56**, 250-256.
18. B. S. Sekhon, *Asian J. Pharm. Biol. Res.*, 2011, **1**, 15.
19. W. L. Hough and R. D. Rogers, *B Chem Soc Jpn*, 2007, **80**, 2262-2269.
20. L. Cammarata, S. G. Kazarian, P. A. Salter and T. Welton, *Phys Chem Chem Phys*, 2001, **3**, 5192-5200.
21. A. Rockenbauer and L. Korecz, *Appl Magn Reson*, 1996, **10**, 29-43.
22. P. He, H. T. Liu, Z. Y. Li, Y. Liu, X. D. Xu and J. H. Li, *Langmuir*, 2004, **20**, 10260-10267.
23. S. Eugenio, C. M. Rangel, R. Vilar and S. Quaresma, *Electrochim Acta*, 2011, **56**, 10347-10352.
24. S. S. Moganty, R. E. Baltus and D. Roy, *Chem Phys Lett*, 2009, **483**, 90-94.
25. L. Xiao and K. E. Johnson, *J Electrochem Soc*, 2003, **150**, E307-E311.
26. L. Yu, H. Sun, J. He, D. Wang, X. Jin, X. Hu and G. Z. Chen, *Electrochemistry Communications*, 2007, **9**, 1374-1381.
27. P. Y. Chen and Y. T. Chang, *Electrochim Acta*, 2012, **75**, 339-346.
28. E. P. Grishina, A. M. Pimenova, N. O. Kudryakova and L. M. Ramenskaya, *Russ J Electrochem+*, 2012, **48**, 1166-1170.
29. F. Endres, *Chemphyschem*, 2002, **3**, 144-+.
30. T. I. Leong, I. W. Sun, M. J. Deng, C. M. Wu and P. Y. Chen, *J Electrochem Soc*, 2008, **155**, F55-F60.
31. H. J. Sun, L. P. Yu, X. B. Jin, X. H. Hu, D. H. Wang and G. Z. Chen, *Electrochemistry Communications*, 2005, **7**, 685-691.
32. A. B. P. Lever, *Inorg Chem*, 1991, **30**, 1980-1985.
33. A. B. P. Lever, *Inorg Chem*, 1990, **29**, 1271-1285.
34. <http://www.chem.yorku.ca/profs/lever/elparameter98.htm>.
35. L. E. Barrosse-Antle, A. M. Bond, R. G. Compton, A. M. O'Mahony, E. I. Rogers and D. S. Silvester, *Chem-Asian J*, 2010, **5**, 202-230.
36. L. H. J. Xiong, A. M. Fletcher, S. G. Davies, S. E. Norman, C. Hardacre and R. G. Compton, *Chem Commun*, 2012, **48**, 5784-5786.
37. A. A. J. Torriero and P. C. Howlett, *Electrochemistry Communications*, 2012, **16**, 84-87.

---

[<sup>i</sup>] P.-Y. Chen, I.-W. Sun, *Electrochim. Acta* 45 (1999) 441-450.

[<sup>ii</sup>] P.-Y. Chen, Chang, *Electrochim. Acta* 75 (2012) 339-346.

[<sup>iii</sup>] E. P. Grishina, A. M. Pimenova, N. O. Kudryakova, L. Ramenskaya, *Russ. J. Electrochem.*, 48 (2012) 1166-1170.

[<sup>iv</sup>] F. Endres, *Chem. Phys. Chem.* 3 (2002) 144-154.